# Photodecomposition of Adsorbed 2-Chloroethyl Ethyl Sulfide on $TiO_2$: Involvement of Lattice Oxygen

**Tracy L. Thompson, Dimitar A. Panayotov, and John T. Yates, Jr.***

*Surface Science Center, Department of Chemistry, University of Pittsburgh, Pittsburgh, Pennsylvania 15260*

**Igor Martyanov and Kenneth Klabunde**

*Department of Chemistry, Kansas State University, Manhattan, Kansas 66506*

*Received: June 30, 2004; In Final Form: August 18, 2004*

The photodecomposition of chemisorbed 2-chloroethyl ethyl sulfide (2-CEES) on the $TiO_2$ surface was investigated using several experimental methods involving both a rutile $TiO_2$(110) surface and powdered P-25 Degussa $TiO_2$. It is found that photooxidation of 2-CEES occurs in the absence of gas-phase oxygen. The oxygen for this process is supplied by the $TiO_2$ lattice. For UV irradiation in the range 3.0−5.0 eV, two simultaneous photodecomposition pathways are measured: one fast process with a measured cross section of $7.4 \times 10^{-19}$ cm$^2$ and one slow process with a measured cross section of $5.4 \times 10^{-20}$ cm$^2$. These two photodecomposition pathways probably involve different modes of binding of the 2-CEES molecule to sites on the $TiO_2$(110) surface. Aldehydic adsorbed products are observed to be produced by UV irradiation and are measured by surface-sensitive IR spectroscopy. In addition, adsorbed carboxylates and carbonates are also produced. GC−MS studies of the gas-phase photodecomposition products produced in the absence of $O_2$ also indicate the production of similar oxygenated products upon UV irradiation of 2-CEES over $TiO_2$ powder as well as many products characteristic of free radical initiated processes on the $TiO_2$ surface. We postulate that free radical species, produced from the 2-CEES molecules by electron or hole attack, are able, in a sequence of reactions, to extract lattice oxygen from the $TiO_2$ photocatalyst surface.

## I. Introduction

The level of interest in the study of photocatalysis over metal oxide materials, specifically titanium dioxide, has grown significantly over recent years, sparked by the use of these materials for environmental cleanup. Materials like titanium dioxide are generally inexpensive, nontoxic, and renewable as catalysts and, for these reasons, are becoming more widespread in their range of applications.[1,2] Titanium dioxide shows promise in this area using sunlight for activation and has been shown to photooxidize a number of pollutants effectively.[3,4]

Traditionally, the study of photocatalysis over titanium dioxide involves either coadsorption of molecular oxygen with an adsorbed molecule or photocatalysis is done under a partial pressure of oxygen. In these instances, molecular oxygen is thought of as an active electron scavenger which effectively accepts electrons available at the surface when the oxide is reduced via thermal treatment or by electron−hole pair creation with UV light.[5] In the results presented here, we look specifically at the interaction of UV radiation with an adsorbed organic molecule (2-chloroethyl ethyl sulfide, 2-CEES) in the *absence* of gas-phase or adsorbed molecular oxygen. The UV-activated surface alone activates the organic molecule, causing it to dissociate. It has been reported that photocatalytic decomposition of acetic[6,7] and formic[8] acids and $CH_2Cl_2$[9] in the absence of gas-phase $O_2$ can proceed on the $TiO_2$ surface under low-intensity UV light exposure, utilizing lattice oxygen as a reactant. In addition, $CH_3CN$ photochemistry on $TiO_2$ has been shown to produce adsorbed NCO species.[10]

The 2-CEES molecule chosen for this work is regularly used as a simulant for the chemical agent, mustard gas. The 2-CEES molecule differs from the actual chemical agent in that it carries only one chlorine atom compared to the dichloro species which is mustard gas. A relatively small amount of research has been done regarding the interaction of this molecule with surfaces. The photooxidation of 2-CEES over titanium dioxide or mixed $TiO_2$−$SiO_2$ has been investigated recently.[11,12]

Panayotov et al. have recently studied the adsorption as well as photooxidation of 2-CEES on mixed $TiO_2$−$SiO_2$ powders.[12,13] The 2-CEES binds via hydrogen bonding through both the chlorine moiety as well as the sulfur atom in the molecule to surface Si−OH groups in the $TiO_2$−$SiO_2$ mixed oxide. Similar surface bonding to Ti−OH groups is observed for $TiO_2$ surfaces.[13] In addition, the photooxidation capabilities (involving $O_2$(g)) of the mixed oxide catalyst toward 2-CEES as well as diethyl sulfide (DES) are reported.[12] For both 2-CEES and DES in the presence of oxygen and UV light, a combination of partially oxidized and fully oxidized products was found on the surface. Martyanov and Klabunde also report clear evidence for a photooxidation reaction of 2-CEES in the presence of oxygen gas and propose a mechanism for photooxidation which involves the presence of the surface hydroxyl radical.[11] Vorontsov et al. have also suggested possible routes for the photooxidation of a similar molecule (DES).[14,15]

The results presented hereafter are from a combined study utilizing ultrahigh-vacuum techniques where experiments are conducted with an atomically clean single-crystal $TiO_2$(110) sample as well as high-vacuum conditions where polycrystalline $TiO_2$ powder is probed using transmission infrared spectroscopy and GC−MS chemical analysis. The use of a single crystal under well-defined UHV conditions allows for very accurate

10.1021/jp040468e CCC: $27.50 
Published on Web 10/26/2004

control of adsorbate exposures as well as complete control of the surface preparation. For studies on structurally undefined $TiO_2$ surfaces, infrared spectroscopy and GC-MS product analysis from powdered $TiO_2$ give chemical insight into the bond-breaking and bond-formation steps associated with the photochemistry.

## II. Experimental Section

The experimental results presented in this paper were carried out in three separate apparatuses. Ultrahigh-vacuum studies of a $TiO_2$(110) crystal have been combined with transmission IR studies and GC−MS product analysis studies of $TiO_2$ powder.

**A. Ultrahigh-Vacuum Study of 2-CEES on $TiO_2$(110).** Experiments involving the photodepletion of 2-chloroethyl ethyl sulfide over $TiO_2$(110) were carried out in a stainless steel ultrahigh-vacuum (UHV) chamber with a base pressure of $<1.5 \times 10^{-10}$ Torr as described previously.[16] For these particular experiments, the chamber is pumped via a turbo molecular pump and a titanium sublimation pump (TSP) in conjunction with a cryoshroud that encircles the lower half of the chamber. The chamber houses an $Ar^+$ sputtering gun to clean the surface, an Auger spectrometer for surface analysis, and a differentially pumped and shielded quadrupole mass spectrometer for both residual gas analysis and for monitoring the change in partial pressure of products desorbing from the front surface of the crystal by direct line-of-sight sampling. The chamber is also equipped with a collimated molecular beam doser for accurate gas exposures. For experiments with 2-CEES, it was found that more consistent and reproducible behavior was obtained when exposing the gas to the $TiO_2$(110) surface via a backfilling method.

The $TiO_2$ single crystal used for this investigation (Princeton Scientific Corp.) measures 10 mm × 10 mm × 1 mm and has slots precut around all four edges for mounting purposes. Clips made of thin tantalum foil insert into each of the four edges in order to tightly hold the $TiO_2$(110) crystal to a tantalum plate of the same size as the crystal. The tantalum plate is then electrically heated and cooled via two tungsten wires that are spot-welded to the back of the tantalum plate. A thermocouple is cemented into one corner slot of the $TiO_2$ crystal for direct temperature measurements.[17]

Crystal preparation is accomplished via cycles of $Ar^+$ sputtering (1500 eV, $I/A = 2\ \mu A/cm^2$, 40 min) and annealing to 900 K in vacuum. Once clean, the defect-free surface is restored by annealing the crystal to 900 K in oxygen flux via the molecular beam doser. The crystal is cooled in the same flux. Once oxidized, the surface is again reduced by annealing in vacuum to 900 K in order to obtain 8−10% oxygen vacancies.[18] The defect density of the crystal was tested using a probe developed in this laboratory that involves the thermal desorption of $CO_2$ from the defective surface.[19] Using this method, as well as testing for the photodesorption of adsorbed $O_2$,[20] we have concluded that the surface is indeed reduced after following the procedures mentioned.

A 500 W Hg Arc lamp (Oriel) was used as the UV source for the single crystal experiments presented. The lamp is equipped with a two-element UV fused silica condensing lens, a water filter, and an iris. The UV light beam is focused on the sample at an angle of approximately 60° to the surface normal. This factor is taken into account when calculating the overall light fluence. The full arc of the lamp was used in order to obtain maximum power for these experiments. The measured power in the photon energy range 3.0−5.0 eV during the experiment was 63 mW/cm$^2$. The "low" light power setting, obtained by adjusting the condensing lens on the lamp, allowed for a power density of 10.7 mW/cm$^2$. The total photon flux is measured during each light exposure by reflecting 10% of the light beam directly to a power meter (Thorlabs, model D10MM). Power densities obtained from this power meter were cross-checked against a thermopile (Oriel, model 71751) and were found to be within 10% of one another. To obtain the approximate photon flux incident on the crystal surface, the average wavelength of the complete lamp irradiance profile was estimated by integration of the lamp profile vs wavelength for energies greater than the band gap of $TiO_2$ in the range from 3.0 to 5.0 eV. This corresponds to an approximate photon flux for the high power setting of $1.02 \times 10^{17}$ photons/(cm$^2$ s) and $1.73 \times 10^{16}$ photons/(cm$^2$ s) for the low power setting.

2-CEES (98%) used in both the UHV and transmission IR studies was obtained from Sigma-Aldrich and further purified via several freeze−pump−thaw cycles. Exposures of 2-CEES to the $TiO_2$(110) surface was done via backfilling the UHV chamber to pressures of $3 \times 10^{-8}$ Torr for various times. When calculating the overall exposure of 2-CEES to the crystal surface, both the ion gauge sensitivity and the contribution of the partial pressure of 2-CEES measured after ending gas admission were considered. The ion gauge sensitivity for 2-CEES is not available in the literature, and therefore an average sensitivity of several similar molecules was taken.[21] The sensitivity ratio $I^+$(2-CEES)/$I^+(N_2) = 2.6$ was employed. Thermal desorption measurements were carried out using a heating rate of 3.0 K/s.

**B. Transmission IR Studies on $TiO_2$ Powder. 1. $TiO_2$ Powder Material.** The $TiO_2$ powder employed for this work is the commonly studied photoactive $TiO_2$ material (Degussa P25). Both the IR and the GC−MS studies used this material. The P-25 $TiO_2$ powder[22] is reported to be 99.5% pure $TiO_2$ (70% anatase and 30% rutile), having a surface area of $50 \pm 15$ m$^2$ g$^{-1}$. The average particle diameter by number count is 21 nm, where 90% of the particles fall in the size range from 9 to 38 nm. The particles exist as aggregates which are approximately 0.1 mm in diameter.[4] For the IR studies, the $TiO_2$ sample is hydraulically pressed into a tungsten grid as a circular spot 7 mm in diameter, typically weighing 4−4.5 mg (10.4−11.7 mg/cm$^2$). The samples and the grid support assembly are then placed into the dual-beam IR−UV photoreactor and evacuated.

**2. High-Vacuum System and UV Photoreactor for IR Studies.** The details of the experimental setup and photoreactor used for the gas-phase photodegradation of 2-CEES on powder $TiO_2$-based materials have been published elsewhere.[23] The experimental setup consists of four main units: (i) high-vacuum system with gas-vapor-delivery module, (ii) dual beam IR−UV photoreactor, (iii) transmission FTIR spectrometer, and (iv) 350 W Hg arc lamp as an ultraviolet light source.

The stainless steel vacuum system is pumped simultaneously with a Pfeiffer Vacuum 60 L/s turbomolecular pump and a Varian 20 L/s ion pump. The base pressure reached after 24 h baking of system while pumping with both pumps is $\sim 10^{-8}$ Torr, as measured by the ionization gauge. The pressure of reactant gases and vapors was measured with a MKS capacitance manometer (Baratron, type 116A, range $10^{-3}$−$10^3$ Torr).

The dual-beam IR−UV photoreactor used in these experiments has been described previously.[23] The stainless steel photoreactor is capable of working under a wide range of pressures ($10^{-8}$ to ~750 Torr) and temperatures (100−1500 K).[24] The powdered $TiO_2$ sample is pressed hydraulically at 12 000 lb/in.$^2$ into the openings of a flat tungsten grid[25] (0.0508 mm thick, with 0.22 mm$^2$ square holes, obtained from Buckbee-

Mears, St. Paul, MN). The grid is held rigidly to a power/thermocouple feedthrough via a pair of nickel clamps and is oriented at a 45° angle to both the IR and the UV beams. The sample temperature is measured using a type K thermocouple spot-welded to the top-center region of the grid. The sample is uniformly heated using the electrical resistance of the tungsten grid. The power leads and the type K thermocouple leads pass through a reentrant Dewar and are connected to a power supply controlled by a Honeywell digital controller. Two different cooling agents (liquid $N_2$ or a mixture of dry ice + acetone) were used to fill the Dewar and cool the sample. The dry ice + acetone mixture was utilized in the experiments carried out at 255 K. The accuracy of the temperature control was ±1 K. The middle and the lower positions on the tungsten grid are used as sample spots. The $TiO_2$ sample pressed onto the lower spot serves as a direct measure of the reproducibility between experiments. The upper position on the grid is empty and is used for the background absorbance measurements in the same experiment. Different positions on the same grid can be aligned to the IR beam using a computer-controlled translation system[26] (Newport Corp.) with ±1 $\mu$m accuracy in both the horizontal and vertical directions.

Infrared spectra were obtained with a nitrogen-gas purged Mattson Fourier transform infrared spectrometer (Research Series I) equipped with a liquid $N_2$ cooled HgCdTe detector. All scans in the infrared region from 4000 to 500 $cm^{-1}$ were made in the ratio mode at a resolution of 4 $cm^{-1}$. Typically, 2000 scans were accumulated in each spectrum to ensure measurement of low-absorbance bands with high signal-to-noise ratio. WinFIRST software supplied by Mattson was used for setting the spectrometer and for spectra acquisition.

The UV light source employed here is a high-pressure 350 W Hg arc (Oriel Corp.) lamp similar to that used in the single crystal work. The lamp is equipped with a water filter to remove the IR radiation. The UV light beam was focused onto the sample through a sapphire window. The intensity of the UV radiation on the sample was 370 mW/$cm^2$ in the energy range 3.0−5.0 eV.

**3. $TiO_2$ Activation. 2-CEES Adsorption and Photodecomposition Experiments.** Consecutive oxidation and thermal reduction procedures are applied for initial activation of a fresh $TiO_2$ sample. The $TiO_2$ sample was heated in vacuum to the desired pretreatment temperature, 675 K, at a rate of 20 K/min, and then treated in vacuum at this temperature for 4 h followed by cooling to room temperature. Oxygen gas at 6 Torr was introduced into the cell, and the temperature was raised again to 675 K at the same rate. After 1 h of oxidation, the sample was cooled to room temperature and $O_2$ was evacuated. At this point, the reference spectra for the oxidized sample were acquired. After that, the sample was reduced in vacuum at 822 K for 3 h and then cooled to room temperature, and the reference spectra for the thermally reduced sample were taken. The powdered $TiO_2$ samples, annealed in vacuum at 822 K, retain some isolated Ti−OH groups which are useful in binding 2-CEES to the surface, as shown previously.[13] The reference IR spectra for oxidized and thermally reduced samples were acquired at room temperature.

The photodecomposition of adsorbed 2-CEES was implemented after exposure to 0.15 Torr of 2-CEES at 255 K.

**C. GC-MS Studies on $TiO_2$ Powder.** Quantitative analysis of the products forming on the surface of $TiO_2$ Degussa P25 was carried out as follows. First, ca. 200 $\mu$L of a suspension of $TiO_2$ in acetone (40 g/L) was deposited on the wall of a quartz cell equipped with a high-vacuum valve. After drying at 323 K in air, the traces of organics on the surface of $TiO_2$ were burned off in air with a full arc of a 1000 W Hg (Xe) lamp. Later, ca. 20 $\mu$L of 2-CEES was added and frozen by immersing the cell in liquid nitrogen followed by evacuation to $10^{-4}$ mbar. Three freeze−pump−thaw cycles were employed to ensure thorough deoxygenation. Following this purification, the cell was sealed and transferred to conduct the photoreaction in the absence of $O_2$.

A 1000 W Hg (Xe) lamp (Oriel) was used to carry out the photoprocess. Before reaching the sample, the light was passed through a water filter and a set of color filters (#57396, 59062 from Oriel) to eliminate IR radiation. The intensity of the light was ~70 mW/$cm^2$ with the UV spectral range being 3.1−4.0 eV.

After 60 min, the illumination was interrupted. The gas in the cell was equilibrated with 1 atm of argon gas. Identification of reaction products was carried out using a GC−MS (QP5000 from Shimadzu) equipped with a capillary column (XTI-5, Rastek Corp.). During the analysis, the temperature of the column was programmed (1 min at 313 K, ramp to 593 K at 40 K/min, and 4 min at 593 K). Nonvolatile products were extracted from the surface of the $TiO_2$ powder with liquid acetonitrile and analyzed in a similar way but with an appropriate cutoff time. To enhance thermal stability and volatility of some of the products in the extract, initial derivatization was done at 323 K for 60 min with a mixture of bis(trimethylsilyl)-trifluoroacetamide with trimethylchlorosilane (BSTFA/TMCS, 99:1, Supelco) and then identified through a similar analytical approach in a separate set of experiments.

## III. Results

**A. Single Crystalline $TiO_2$. 1. Thermal Desorption of 2-CEES from $TiO_2$(110).** The thermal chemistry of 2-CEES adsorbed on $TiO_2$(110) is thoroughly discussed elsewhere.[16] Briefly, in adsorption experiments beginning at 110 K, it was found that 2-CEES thermally decomposes during the thermal desorption of the parent 2-CEES molecule in the temperature range from 110 to 800 K. Auger analysis of the surface after the thermal desorption of the parent 2-CEES molecule by heating to a temperature of 500 K shows that the surface is contaminated with S, Cl, and C. From these results, we estimate that approximately 20% of the initial coverage of 2-CEES is thermally decomposed upon heating to 500 K.[16]

**2. Photodecomposition of 2-CEES on $TiO_2$(110) in Vacuum.** Figure 1 shows the result of the exposure of UV light to the adsorbed 2-CEES/$TiO_2$(110) system. For these experiments an initial coverage of 0.5 ML was used. After adsorption of 2-CEES at 110 K, the crystal was exposed to full arc irradiation (63 mW/$cm^2$ = 1.02 × $10^{17}$ photons/($cm^2$ s)) for a certain time period, followed by temperature-programmed desorption (TPD) to monitor the change in the amount of adsorbed 2-CEES due to photodecomposition. The major mass spectrometer cracking product of the 2-CEES molecule at 75 amu was monitored. Experiments were also done using a lower light power setting (10.7 mW/$cm^2$ = 1.73 × $10^{16}$ photons/($cm^2$ s)) in order to more accurately measure the photodecomposition effect at lower light fluences. During UV exposure, the crystal temperature increased no more than 5 K. The inset to Figure 1 shows an example of the actual TPD data where there is evidence of a large decrease in the amount of remaining 2-CEES after 60 s (6.1 × $10^{18}$ photons/$cm^2$) of exposure to UV light as compared to measurements made on the nonirradiated surface. For increasing UV exposure times, the amount of adsorbed 2-CEES decreased monotonically. The decrease in 2-CEES coverage was fit to a

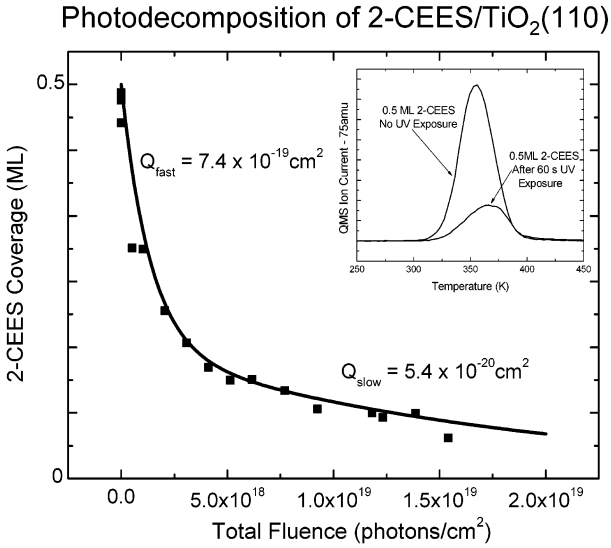


**Figure 1.** Measurement of the decrease in the TPD peak area of adsorbed 2-CEES with increasing photon fluence. Fitting of the experimental data shows two simultaneous processes which occur, each with a different cross section.

double-exponential decay rate as shown in Figure 1. Total cross sections for both the fast and slow photodecomposition process were measured to be $Q_{fast} = 7.4 \times 10^{-19}$ cm$^2$ and $Q_{slow} = 5.4 \times 10^{-20}$ cm$^2$, and the fitted curve corresponds to these two parallel processes. Upon completion of thermal desorption to 900 K, the surface became clean, and its ability to adsorb 2-CEES was fully restored.

The measurements of the two photodecomposition cross sections for 2-CEES are confounded by a small thermal decomposition process which occurs during the TPD measurement. The 20% thermal decomposition that occurs during each measurement has a direct effect on the measured coverage.[16] However, this effect does not influence our evaluation of the magnitude of the total measured cross sections for the photo-induced decomposition of 2-CEES in the two processes found in this work.

To ensure that the 2-CEES molecule was in fact decomposed, and not just photodesorbed, an experiment was done by monitoring mass 75 during the initial exposure to UV using direct line-of-sight sampling by the mass spectrometer. Results of that experiment are shown in Figure 2a where there is no photodesorption signal detected above the noise level. Figure 2b shows the expected photodesorption signal for 0.03 monolayers of 2-CEES. The assumed photodesorption cross section for this simulation is $7.4 \times 10^{-19}$ cm$^2$, consistent with the measurements in Figure 1. The comparison of parts a and b of Figure 2 clearly shows that much less than 0.03 ML photodesorption of the 2-CEES molecule occurs. We therefore conclude that the photodepletion effect is indeed due almost exclusively to UV-induced photodecomposition of the 2-CEES molecule.

**B. Powdered $TiO_2$ Results: IR Spectroscopy. 1. Adsorption of 2-CEES on $TiO_2$ Powder.** The adsorption of 2-CEES on $TiO_2$ Degussa P25 powder is discussed elsewhere.[16] Briefly, it was found that adsorption of 2-CEES on high area anatase powder at 255 K produces IR absorption bands in the regions of both the $\nu(CH_x)$ stretching (3000−2700 cm$^{-1}$) and the $\delta(CH_x)$ deformation (1500−1000 cm$^{-1}$) modes which are characteristic of the adsorbed molecule. In addition, all types of isolated Ti−OH groups[16,27−29] interact via hydrogen bonding with the adsorbed 2-CEES molecule.[16] The loss of isolated Ti−OH

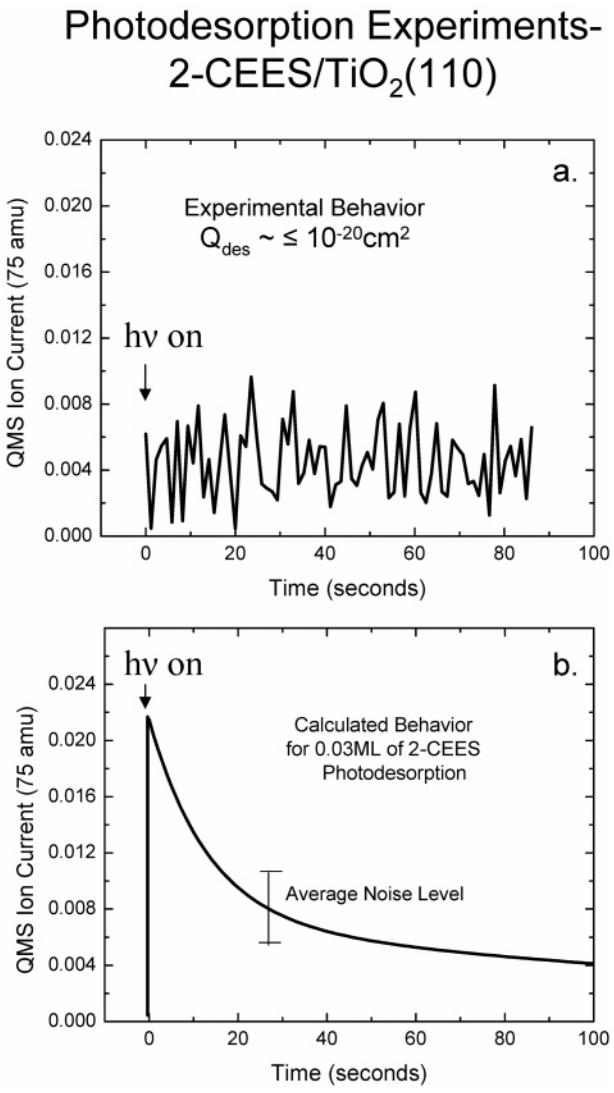


**Figure 2.** (A) Measurement of the lack of observed photodesorption of the parent 2-CEES molecule. (B) Simulated curve for the expected photodesorption of 2-CEES. The simulation intensity is for the desorption of 0.03 ML of 2-CEES, corresponding to a photodesorption cross section of $4.4 \times 10^{-20}$ cm$^2$.

groups during 2-CEES adsorption is accompanied by the production of a number of types of associated Ti−OH groups which exhibit lower OH stretching frequencies. The hydrogen bonding of 2-CEES to Ti−OH groups keeps the molecule strongly bonded to the $TiO_2$ surface, and it is not desorbed at 255 K under dynamic high vacuum conditions, as reported previously.[16] It is likely that 2-CEES also bonds to other sites on the partially dehydroxylated $TiO_2$ surface studied here, as found on the $TiO_2$ single crystal.

**2. IR Measurements of 2-CEES Photodecomposition on $TiO_2$ Powder.** Illumination of 2-CEES-covered $TiO_2$ powder with polychromatic UV light (3.0−5.0 eV, $P = 370$ mW/cm$^2$) at 255 K in vacuum causes a pronounced increase in the background IR absorbance of the $TiO_2$ over the entire region from 3000 to 1000 cm$^{-1}$. Subtraction of the spectrum before the beginning of irradiation from the excited-state spectrum produces a structureless broad IR background absorption which increases with time of UV illumination. Selected background spectra measured as a function of the UV exposure time for the 2-CEES/$TiO_2$ powder system are presented in Figure 3. This physical phenomenon, absorption of light due to mobile charge carriers, was first observed for silicon[30,31] and germanium.[32,33]

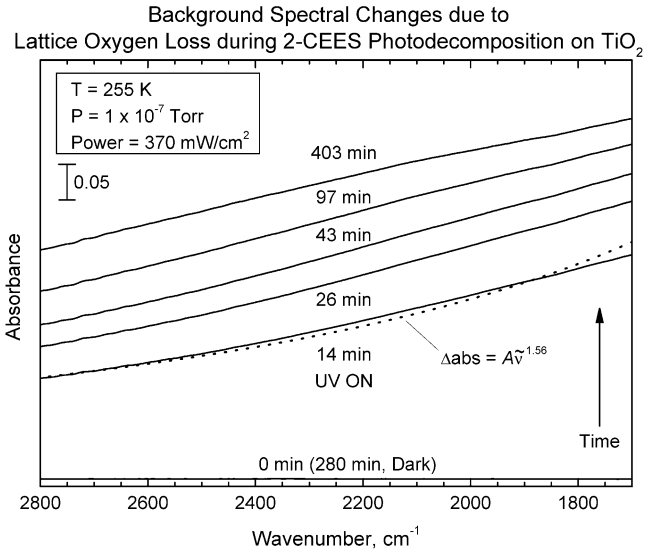


**Figure 3.** Change in the IR absorbance due to the loss of lattice oxygen as a function of UV exposure during 2-CEES decomposition. The depicted increase in the background IR absorbance signifies the presence of mobile electrons in the conduction band as a result of UV excitation.

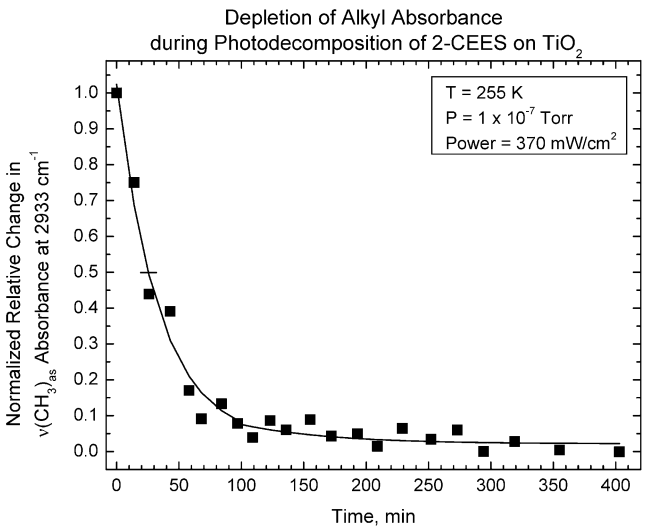


**Figure 4.** Loss of alkyl absorbance with increasing UV exposure measured by IR spectroscopy during 2-CEES photodecomposition.

Theories on the transport process for conduction electrons have also been developed.[34−36] The change in the background IR absorption is caused by the formation of electron traps due to the loss of lattice oxygen and their filling by electrons near the conduction band edge. This effect has been well studied by others[37−43] as well as by ourselves.[16,44,45] A broad and structureless IR absorption has also been reported for $TiO_2$ after UV excitation and is assigned to continuous charge carrier transitions into the conduction band specific to semiconductors.[40−43] The signal growth with a $\sim\nu^{-1.5}$ law is usually observed for electronic interband transitions, where acoustic phonons provide the required momentum.[46] We have recently reported that, during continuous UV irradiation of $TiO_2$ powder in the mW $cm^{-2}$ range, photogenerated electrons are either trapped at localized sites giving paramagnetic $Ti^{3+}$ centers or excited to the conduction band, giving EPR-silent conduction band electrons which may be observed by their structureless IR absorption,[47] as seen in Figure 3. The EPR measurements show that under high-vacuum conditions the majority of photoexcited electrons enter the conduction band.[47]

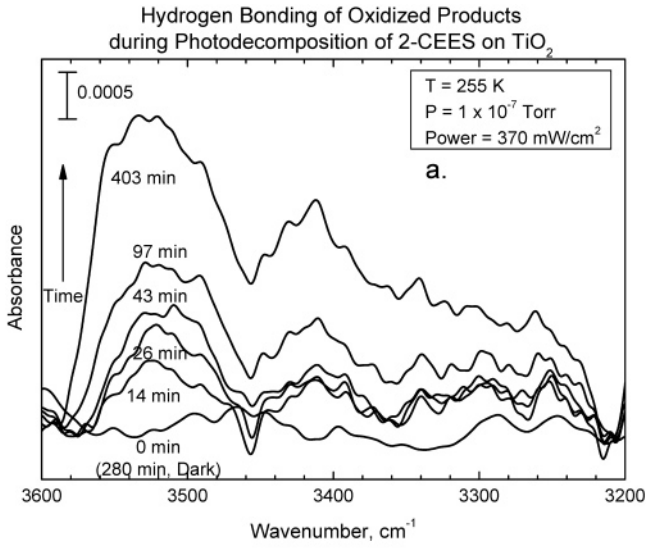


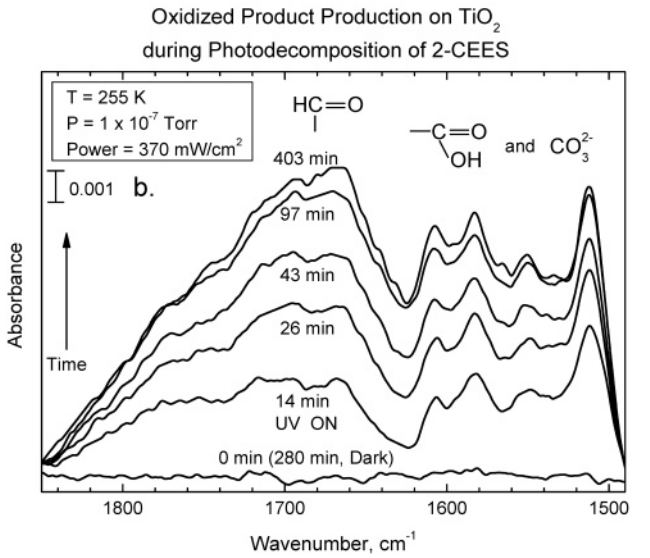


**Figure 5.** Formation of hydrogen-bonded and oxygen-containing products with increasing UV exposure during 2-CEES photodecomposition.

Thus, the increase in the background absorbance during UV irradiation of $TiO_2$ covered by adsorbed 2-CEES (as shown in Figure 3) can be attributed to loss of lattice oxygen and to the concomitant photoexcitation of electrons into the trap sites produced near the conduction band edge.

**3. Photodecomposition of 2-CEES on $TiO_2$ Powder in Vacuum.** Figure 4 shows the kinetics of absorbance change due to alkyl group depletion as a result of the exposure to UV light of the 2-CEES /$TiO_2$ powder system. During UV exposure, the sample temperature was controlled and did not exceed 255 K. The total photodecomposition of 2-CEES, estimated on the basis of the integrated alkyl absorbance within the range 3010−2820 $cm^{-1}$, was about 5% of the initial 2-CEES coverage.

**4. Formation of Oxidized Products during Photodecomposition of 2-CEES.** The formation of oxidized products and their hydrogen bonding to surface Ti−OH groups is observed during UV exposure of 2-CEES on $TiO_2$ powder in vacuum as shown in Figure 5. The difference spectra in Figure 5a,b show the growth of IR features due to (a) associated Ti−OH groups ($\sim$3530 $cm^{-1}$) and (b) carbonyl stretching modes (1500−1760 $cm^{-1}$). The broad IR absorption band centered at 1680 $cm^{-1}$ (Figure 5b) is attributed to various carbonyl stretching modes due to aldehyde species, while the IR features below 1620 $cm^{-1}$

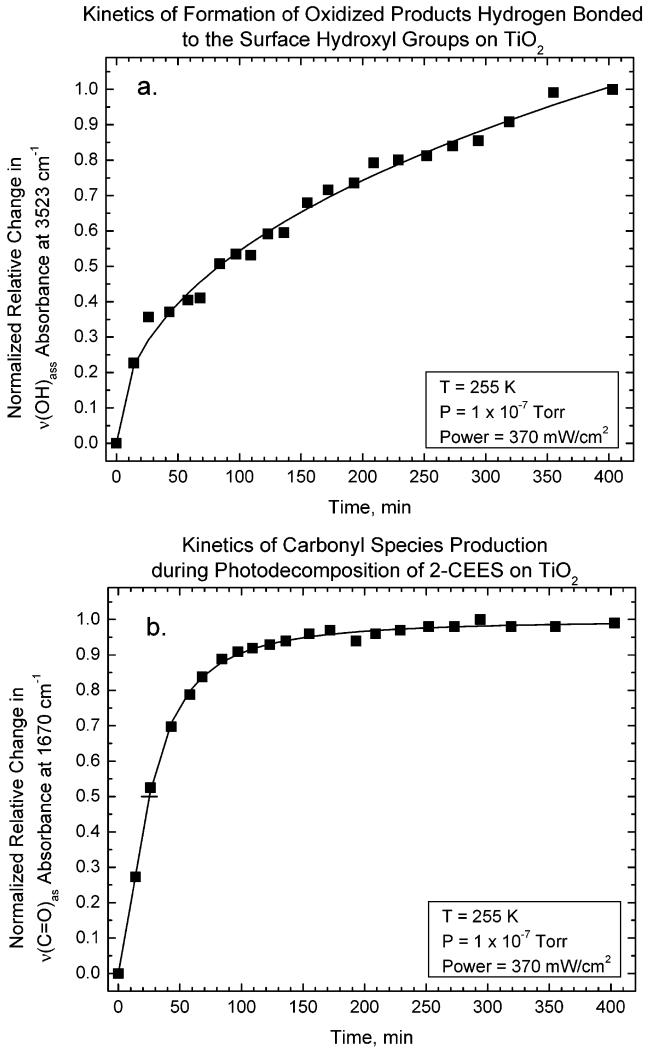


**Figure 6.** Measured kinetics for the formation of products as a result of UV radiation for both hydrogen bonded and other oxygenated products.

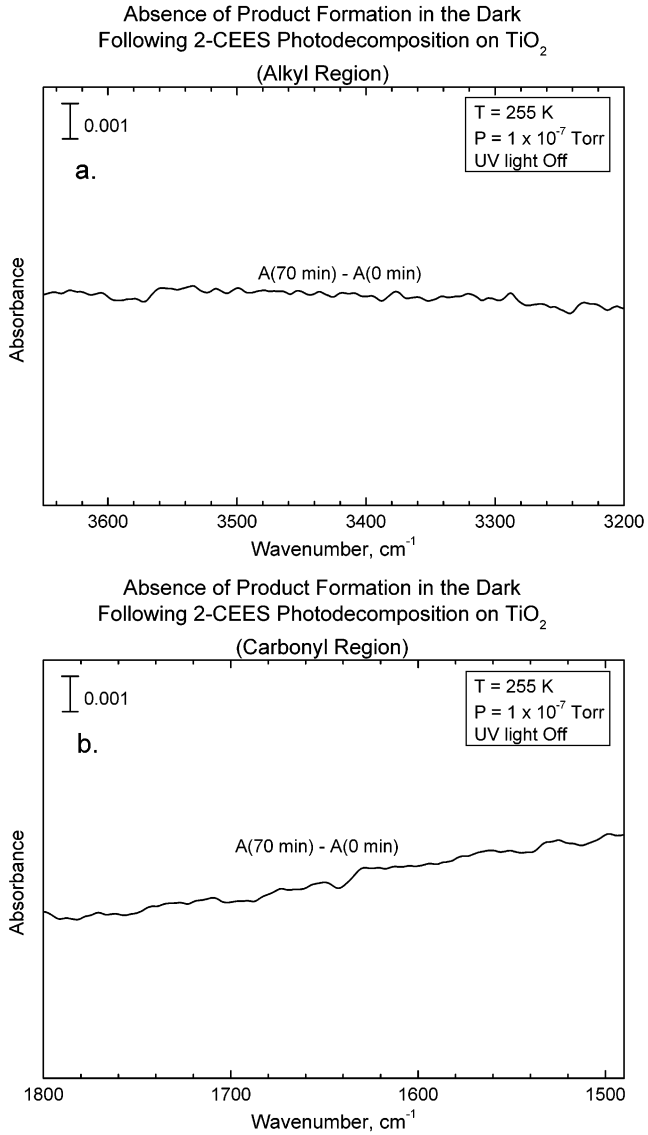


**Figure 7.** Absence of additional 2-CEES degradation in the dark.

are due to various carboxylate and carbonate species. As the oxidized products are formed, they are hydrogen bonded to surface Ti−OH groups that produce the broad IR absorption in the region from 3600 to 3200 $cm^{-1}$ (Figure 5a) where hydroxyl groups associated with oxidation products are reported to absorb.[16,27,28] The changes in the spectrum of adsorbed 2-CEES reveal the photodissociation process of the parent 2-CEES molecule. Analogous spectral changes to those presented in Figure 5 have recently been reported for the photocatalytic oxidation of 2-CEES in the presence of $O_2$ on $TiO_2-SiO_2$ powder.[12] Aldehydes are the primary gas products for 2-CEES[11] and DES[15] photocatalytic oxidation in the presence of $O_2$(g) on $TiO_2$ powder. As our photoillumination experiments with the 2-CEES/$TiO_2$ powder system are performed under high-vacuum conditions at a base pressure of $1 \times 10^{-7}$ Torr, i.e., in absence of gas-phase oxygen, oxidized products can be produced only at the expense of the $TiO_2$ lattice oxygen. The removal of lattice oxygen due to supra-band-gap photoexcitation of the $TiO_2$ powder containing chemisorbed 2-CEES is detected indirectly by the changes in the background IR absorption of the catalyst sample, as shown in Figure 3. Therefore, the oxidative photodegradation of 2-CEES adsorbed on $TiO_2$ involves the lattice oxygen of $TiO_2$.

**5. Selected Kinetics Results for 2-CEES Photodecomposition Using Infrared Absorbances.** Figure 6 shows the rates of photodecomposition as observed from the changes in infrared absorbances of 2-CEES on $TiO_2$ at 255 K. Figure 6a presents the kinetics for the growth in intensity of hydrogen-bonded hydroxyls as measured by the absorbance at 3523 $cm^{-1}$ (Figure 5a). The kinetics of aldehyde species production is shown in Figure 6b and is measured by the absorbance at 1670 $cm^{-1}$. A comparison of the kinetics of aldehyde species formation (Figure 6b) with that for 2-CEES depletion (Figure 4) clearly reveals the correspondence between the two processes; as 2-CEES is photodecomposed, aldehyde species are produced with approximately the same kinetics ($\tau_{1/2} \approx 25$ min). This correlation implies that the photodepletion of 2-CEES is directly related to the formation of aldehydes, i.e., the oxidative photodegradation of 2-CEES involving lattice oxygen is the main photocatalytic process on the $TiO_2$ surface. The kinetics of hydrogen-bonded species production (Figure 6a) is retarded compared to the formation of the aldehyde products, possibly because some of these products originate from subsequent oxidation steps beyond the aldehyde stage.

**6. Absence of Reactivity after Switching from UV Illumination to Dark Conditions.** The results presented in Figure 7 show that after switching off the UV source no further spectral changes are observed for 70 min under dark conditions in vacuum. This means that no further thermal processes take place

**TABLE 1: Relative Amounts of the Products of the Photoreaction of 2-CEES on $TiO_2$ Detected in the Gas Phase**

| product | | % |
|---|---|---|
| hydrogen chloride | HCl | 16 |
| carbon dioxide | $CO_2$ | 15 |
| ethylene | $C_2H_4$ | 10 |
| chloroethylene | $ClCHCH_2$ | 1.3 |
| acetaldehyde | $CH_3C(O)H$ | 8.5 |
| chloroethane | $ClCH_2CH_3$ | 3.7 |
| ethanethiol | $CH_3CH_2SH$ | 18 |
| dichloromethane | $CH_2Cl_2$ | 12 |
| ethyl methyl sulfide | $CH_3CH_2SCH_3$ | 3 |
| 1,2-dichloroethane | $ClCH_2CH_2Cl$ | 0.4 |
| ethyl vinyl sulfide | $CH_3CH_2SCHCH_2$ | 9.8 |
| diethyl disulfide | $CH_3CH_2SSCH_2CH_3$ | 1.7 |
| 1,2-bis(ethylthio)ethane | $CH_3CH_2SCH_2CH_2SCH_2CH_3$ | 0.6 |

at 255 K, and thus, the photooxidation of 2-CEES by lattice oxygen is not likely to involve a thermal process at 255 K which operates in parallel with the photodecomposition process. It was also found that under dark conditions no further changes in the background IR absorption take place (not shown); i.e., the background does not relax to the state measured before UV irradiation. This implies that at 255 K in vacuum the photoexcited electrons in $TiO_2$ remain trapped in the conduction band (separated from holes) after discontinuation of UV illumination.

**C. Powdered $TiO_2$ Results: GC−MS Studies.** In contrast to the oxidation of 2-CEES over $TiO_2$ in air, the illumination of the $TiO_2$ containing 2-CEES in an oxygen-free environment resulted in the sample's color change from white to light blue. The light blue color is characteristic of the production of slightly reduced $TiO_2$ as lattice oxygen depletion from the bulk occurs during photoreaction.

The set of the products detected in the gas phase and their relative amounts (measured in terms of total ion current measured by the MS detector) are given in Table 1.

Two oxygen-containing products including acetaldehyde ($CH_3C(O)H$) and carbon dioxide ($CO_2$) were found to be formed and released in the gas phase during the photoreaction. The production of these two gas-phase products correlate well with the observation by IR spectroscopy of aldehyde groups and carbonate groups formed on the $TiO_2$ surface (Figure 5b). Other gaseous products of the photodecomposition reaction were found to be oxygen free.

Additionally, five products were detected in the extract from the $TiO_2$ after the photoreaction (Table 2). Two of these five products also contain oxygen derived from the $TiO_2$ lattice.

## IV. Discussion

**A. Photodecomposition of 2-CEES on $TiO_2$(110).** The use of an atomically clean single crystal of $TiO_2$ provides an opportunity to observe photoprocesses on the surface which is not covered by other chemical species. Our studies indicate that the clean $TiO_2$ surface exhibits a high efficiency for inducing the photodecomposition of the 2-CEES molecule. The depletion of the molecule occurs via two parallel processes exhibiting cross sections of $7.4 \times 10^{-19}$ cm$^2$ and $5.4 \times 10^{-20}$ cm$^2$. These cross sections are in the range often observed for the photochemical destruction of molecules on metal and semiconductor surfaces.[48,49] The photochemical destruction process is induced by electron−hole pair formation in the semiconductor and is due to the action of either photogenerated electrons and/or photogenerated holes. In the case of photogenerated electrons, electron attachment processes to adsorbed molecules are often observed in other surface-mediated photochemical systems,[48,50−52] and the temporary negative ion produced then decomposes via a reaction schematically shown in eq 1.

$$RX + e^- \rightarrow RX^- \rightarrow R^\bullet + X^- \rightarrow ... \quad (1)$$

The $R^\bullet$ species, a reactive free radical, can then participate in other chemical steps where it reacts with other RX or $R^\bullet$ species.

A hole generated by electron−hole pair formation in $TiO_2$ may abstract an electron from an adsorbed species to produce a radical cation. As shown in eq 2, the radical cation may also undergo subsequent reaction steps.

$$RX + h^+ \rightarrow RX^{\bullet+} \rightarrow ... \quad (2)$$

In addition to the scission of chemical bonds in an adsorbed molecule induced indirectly by electrons or holes photoproduced in the substrate, it is also possible to induce photodesorption for certain molecules chemisorbed on $TiO_2$ as has been reported previously.[17,53] Our experiments, shown in Figure 2, indicate that the photodesorption channel is nonexistent or of very low cross section for the 2-CEES molecule on $TiO_2$. The measurements in Figure 2 suggest that if photodesorption does occur, the cross section for the process must be below $\sim 10^{-20}$ cm$^2$.

The direct photoexcitation of an adsorbed molecule by absorption of a photon may also induce chemical decomposition. To evaluate the probability of a direct photochemical process, we measured the UV absorbance of a solution of 2-CEES in *n*-hexane (Figure 8). In the photon energy range from 3.2 to 5.0 eV, we measure an average photoabsorption cross section of $2.8 \times 10^{-21}$ cm$^2$. Assuming a quantum efficiency of unity, we calculate that a maximum of ~5% of the 2-CEES monolayer could be decomposed by *direct* UV excitation (photon fluence $= 2 \times 10^{19}$ cm$^{-2}$. On this basis, we conclude that the major contribution to the overall photodecomposition of 2-CEES is substrate mediated.

**B. Reaction of Lattice O in $TiO_2$.** A key finding in this work is that in the absence of $O_2$ the 2-CEES molecule is photooxidized. For this to happen, lattice oxygen must be involved. The presence of high cross section photoreaction processes on $TiO_2$(110), which contains no Ti−OH groups, indicates that the photoreactions of 2-CEES occur without the involvement of Ti−OH groups. Furthermore, when Ti−OH groups are present on the surface, the IR results indicate that they are not consumed in the reaction and that instead they form hydrogen bonds with the reaction products (Figures 5a and 6a). Therefore, under photochemical excitation conditions, these results indicate that the lattice oxygen in $TiO_2$ is labile when an organic molecule such as 2-CEES is photodecomposed by capture of an electron or a hole. Product yield studies, using GC−MS analysis, further indicate that the oxygenated gas-phase products, $CO_2$ and $CH_3C(O)H$, and a surface-bound alcoholic product are formed at ~300 K. Another ether-type product remains on the $TiO_2$ surface (Table 2). The production of these products is consistent with the observation by infrared spectroscopy of surface carbonate ($CO_3^{2-}$) formation and surface carboxylate (COOH) and surface aldehyde (HCO) formation at 255 K under anaerobic photodecomposition conditions over powdered $TiO_2$ (Figure 5b).

One might postulate that UV irradiation of $TiO_2$ could generate oxygen anion vacancy defects, and the liberated oxygen might be a reactive oxidant species. However, careful STM measurements made previously[54] indicate that UV radiation is inactive for producing surface oxygen vacancy defects on $TiO_2$(110).

**TABLE 2: Relative Amounts of the Products of the Photoreaction of 2-CEES on $TiO_2$ Detected in Acetonitrile Extract**

| product | | % |
|---|---|---|
| chloroethyl ethyl disulfide | $ClCH_2CH_2SCH_2CH_3$ | 16 |
| 1,2-bis(ethylthio)ethane | $CH_3CH_2SCH_2CH_2SCH_2CH_3$ | 55 |
| 1-[(2-chloroethyl)thio]-2-(ethylthio)ethane | $ClCH_2CH_2SCH_2CH_2SCH_2CH_3$ | 28 |
| bis[2-(ethylthio)ethyl] ether | $CH_3CH_2SCH_2CH_2OCH_2CH_2SCH_2CH_3$ | 1 |
| 2-hydroxyethyl ethyl sulfide[a] | $CH_3CH_2SCH_2CH_2OH$ | |

[a] This compound was detected only after derivatization as 2-[trimethylsiloxy]ethyl ethyl sulfide ($(CH_3)_3SiOCH_2CH_2SCH_2CH_3$).

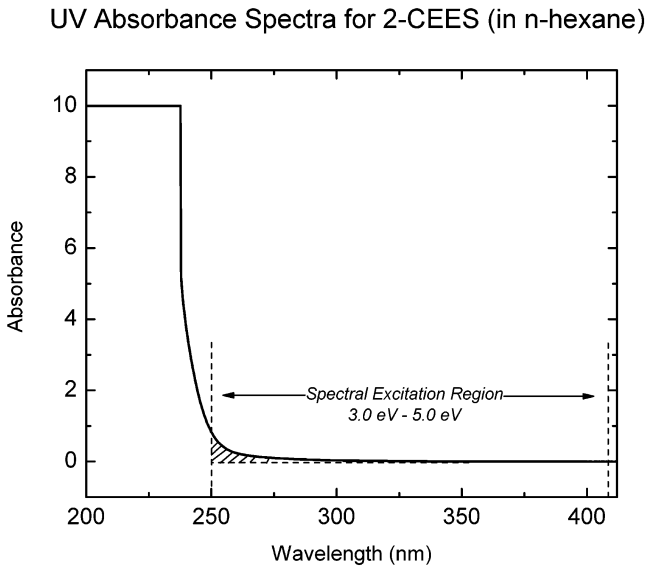


**Figure 8.** UV absorbance spectra for 2-CEES diluted in *n*-hexane. The absorbance at wavelengths above 250 nm may be used to estimate the fraction of incident radiation absorbed by 2-CEES on the $TiO_2(110)$ crystal.

We therefore postulate that reactive organic species, made by either hole attack or electron attachment processes with the 2-CEES molecule, are responsible for the abstraction of lattice oxygen from $TiO_2$. These reactive organic species are most likely free radical species. The reaction may be schematically written as in eq 3 and 4:

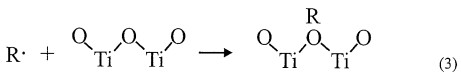


(3)

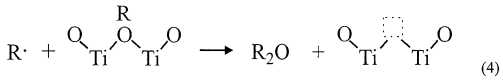


(4)

Thermochemical arguments involving single alkyl ($R^{\bullet}$) radical attack on $TiO_2$(s) and producing a gas-phase RO species lead to highly unfavorable endothermic processes. However, multiple radical attack reactions producing $R_2O$ species may be exothermic and favorable. Most of the products of the photodecomposition of 2-CEES shown in Tables 1 and 2 can only be formed by multiple step elementary processes induced photochemically. A similar radical-induced lattice oxygen abstraction process has been observed for CN radicals produced photochemically on $TiO_2$ where adsorbed NCO species were produced.[10] In addition to multiple radical abstraction processes, the production of carbene species which attack lattice oxygen with favorable thermodynamics is possible, leading for example to aldehyde and $CO_2$ formation.

Further evidence for the removal of lattice oxygen by the photoprocess studied here may be found in the behavior of the infrared background during 2-CEES photodecomposition in the absence of $O_2$. Figure 3 shows that the photoreaction is accompanied by a significant increase in the IR background. This effect is due to the removal of O atoms from the lattice, which leads to the capture of electrons near the conduction band edge. These electrons may be observed by their broadband IR absorbance as a result of electronic excitations occurring into the continuum set of levels available to trapped electrons near the conduction band edge.[34−36,46] Indeed, annealing of $TiO_2$, which also results in oxygen depletion from the surface, and the concomitant trapping of electrons in the conduction band are accompanied by a similar enhancement in the IR background absorbance.[16,40,42−44,47]

**C. Radical Production by Anaerobic Photodecomposition of 2-CEES on $TiO_2$.** Many of the products shown in Tables 1 and 2 are likely to be formed by multiple free radical reactions. For example, the S−S bond in the diethyl disulfide product clearly results from a particular C−S bond cleavage process at the chlorinated ethyl group of the 2-CEES reactant, followed by recombination of the radical products. Similarly, the ethanethiol product must originate from the cleavage of the same C−S bond. Photochemical radical processes resulting in C−C, C−Cl, and C−H bond scission are also indicated by the products observed as listed in Tables 1 and 2.

**D. Connection to Photooxidation Chemistry on $TiO_2$.** During photooxidation processes on $TiO_2$, it is believed that molecular $O_2$ acts as an electron scavenger. Thus, photoreduction processes involving the organic molecule might not be observed in the presence of $O_2$ due to competition by $O_2$ for electrons. Therefore, the comparison of the oxidation products obtained under anaerobic conditions with those obtained in the presence of molecular oxygen[11,12] is informative. The comparison shows that products such as ethyl vinyl sulfide ($CH_3CH_2SCHCH_2$) and HCl are produced primarily in the absence of $O_2$. These particular products may therefore result from electron transfer from $TiO_2$ rather than from hole-induced effects since $O_2$ inhibits their formation.

## V. Summary of Results

The anaerobic photochemical reaction of 2-chloroethyl ethyl sulfide (2-CEES) on the $TiO_2$ surface has been studied using a combination of measurement techniques designed to understand photophysical and photochemical phenomena. The following results have been obtained:

1. Photooxidation of 2-CEES occurs on the $TiO_2$ surface in the absence of added molecular oxygen; the source of the oxygen is the $TiO_2$ lattice.

2. For UV irradiation in the energy range 3.0−5.0 eV, two photoreaction processes occur on $TiO_2(110)$ in parallel with cross sections of $7.4 \times 10^{-19}$ cm$^2$ and $5.4 \times 10^{-20}$ cm$^2$. Photodesorption is not observed and the upper limit of the cross section for 2-CEES photodesorption is $\sim 10^{-20}$ cm$^2$.

3. Indirectly excited photoprocesses which cause the scission of C−S, C−C, C−Cl, and C−H bonds are inferred from the many products observed. These products are associated molecules, most likely produced by a sequence of free radical steps induced when electrons and holes are photogenerated in the $TiO_2$ and transferred to adsorbed 2-CEES molecules.

4. Direct photoexcitation of the adsorbed 2-CEES molecule in the photon energy range 3.0−5.0 eV is excluded on the basis of the minor UV absorbance of the molecule in this range.

5. It is postulated that lattice oxygen extraction from $TiO_2$ is caused by multiple free radical attack processes on the $TiO_2$ surface, where free radical species are generated by electron and/or hole interaction with the adsorbed 2-CEES molecule. Using more than a single free radical to attack the $TiO_2$ can lead to favorable thermodynamics for oxygen extraction from $TiO_2$(s).

**Acknowledgment.** We acknowledge with thanks the support of this work by the DoD Multidisciplinary University Research Initiative (MURI) program administered by the Army Research Office under Grant DAAD 19-01-0-0619.

## References and Notes

(1) Hoffmann, M. R.; Martin, S. T.; Choi, W. Y.; Bahnemann, D. W. *Chem. Rev.* **1995**, *95*, 69−96.
(2) Anpo, M. *Pure Appl. Chem.* **2000**, *72*, 1265−1270.
(3) Anpo, M. *Catal. Surveys Jpn.* **1997**, *1*, 169.
(4) Mills, A.; LeHunte, S. *J. Photochem. Photobiol. A* **1997**, *108*, 1−35.
(5) Linsebigler, A. L.; Lu, G. Q.; Yates Jr., J. T. *Chem. Rev.* **1995**, *95*, 735−758.
(6) Sclafani, A.; Palmisano, L.; Schiavello, M.; Augugliaro, V. *New J. Chem.* **1988**, *12*, 129.
(7) Muggli, D. S.; Falconer, J. L. *J. Catal.* **1999**, *187*, 230−237.
(8) Muggli, D. S.; Falconer, J. L. *J. Catal.* **2000**, *191*, 318−325.
(9) Chen, M. T.; Lien, C. F.; Liao, L. F.; Lin, J. L. *J. Phys. Chem. B* **2003**, *107*, 3837−3843.
(10) Zhuang, J.; Rusu, C. N.; Yates Jr., J. T. *J. Phys. Chem. B* **1999**, *103*, 6957−6967.
(11) Martyanov, I. N.; Klabunde, K. J. *Environ. Sci. Technol.* **2003**, *37*, 3448−3453.
(12) Panayotov, D. A.; Paul, D. K.; Yates Jr., J. T. *J. Phys. Chem. B* **2003**, *107*, 10571−10575.
(13) Panayotov, D.; Yates Jr., J. T. *J. Phys. Chem. B* **2003**, *107*, 10560−10564.
(14) Kozlov, D. V.; Vorontsov, A. V.; Smirniotis, P. G.; Savinov, E. N. *Appl. Catal. B* **2003**, *42*, 77−87.
(15) Vorontsov, A. V.; Savinov, E. V.; Davydov, L.; Smirniotis, P. G. *Appl. Catal. B* **2001**, *32*, 11−24.
(16) Thompson, T. L.; Panayotov, D.; Yates Jr., J. T. *J. Phys. Chem. B*, in press.
(17) Lu, G. Q.; Linsebigler, A.; Yates Jr., J. T. *J. Chem. Phys.* **1995**, *102*, 4657−4662.
(18) Pan, J. M.; Maschhoff, B. L.; Diebold, U.; Madey, T. E. *J. Vac. Sci. Technol. A* **1992**, *10*, 2470−2476.
(19) Thompson, T. L.; Diwald, O.; Yates Jr., J. T. *J. Phys. Chem. B* **2003**, *107*, 11700−11704.
(20) Lu, G. Q.; Linsebigler, A.; Yates Jr., J. T. *J. Phys. Chem.* **1994**, *98*, 11733−11738.
(21) Nakao, F. *Vacuum* **1975**, *25*, 431−435.
(22) Highly Dispersed Mettalic Oxides Produced by Aerosil Process. *Degussa Tech. Bull. Pigments* **1990**, *56*, 13.
(23) Rusu, C. N.; Yates Jr., J. T. *J. Phys. Chem. B* **2000**, *104*, 1729−1737.
(24) Basu, P.; Ballinger, T. H.; Yates Jr., J. T. *Rev. Sci. Instrum.* **1988**, *59*, 1321.
(25) Ballinger, T. H.; Wong, J. C. S.; Yates Jr., J. T. *Langmuir* **1992**, *8*, 1676−1678.
(26) Mawhinney, D. B.; Rossin, J. A.; Gerhart, K.; Yates Jr., J. T. *Langmuir* **1999**, *15*, 4617−4621.
(27) Primet, M.; Pichat, P.; Matthieu, M.-V. *J. Phys. Chem.* **1971**, *75*, 1216.
(28) Tanaka, K.; White, J. M. *J. Phys. Chem.* **1982**, *86*, 4708.
(29) Hadjiivanov, K. I.; Klissurski, D. G. *Chem. Soc. Rev.* **1996**, *25*, 61.
(30) Becker, M.; Fan, H. Y. *Phys. Rev.* **1949**, *76*, 1531−1532.
(31) Briggs, H. B. *Phys. Rev.* **1950**, *77*, 727−728.
(32) Briggs, H. B.; Fletcher, R. C. *Phys. Rev.* **1953**, *91*, 1342−1346.
(33) Harrick, N. J. *Phys. Rev.* **1956**, *97*, 491−492.
(34) Kahn, A. H. *Phys. Rev.* **1955**, *97*, 1647−1652.
(35) Spitzer, W. G.; Fan, H. Y. *Phys. Rev.* **1957**, *106*, 882−890.
(36) Meyer, H. J. G. *Phys. Rev.* **1958**, *1958*, 298−308.
(37) Baratron, M.-I.; Merhari, L. *Scr. Mater.* **2001**, *44*, 1643−1648.
(38) Baratron, M.-I.; Merhari, L. *Eur. Ceram. Soc.* **2004**, *24*, 1399−1404.
(39) Ghiotti, G.; Chiorino, A.; Boccuzzi, F. *Surf. Sci.* **1993**, *287*, 228−234.
(40) Szczepankiewicz, S. H.; Colussi, A. J.; Hoffmann, M. R. *J. Phys. Chem. B* **2000**, *104*, 9842−9850.
(41) Yamakata, A.; Ishibashi, T.; Onishi, H. *J. Phys. Chem. B* **2001**, *105*, 7258−7262.
(42) Szczepankiewicz, S. H.; Moss, J. A.; Hoffmann, M. R. *J. Phys. Chem. B* **2002**, *106*, 7654−7658.
(43) Szczepankiewicz, S. H.; Moss, J. A.; Hoffmann, M. R. *J. Phys. Chem. B* **2002**, *106*, 2922−2927.
(44) Panayotov, D.; Yates Jr., J. T. *Chem. Phys. Lett.* **2003**, *381*, 154−162.
(45) Panayotov, D.; Yates Jr., J. T. *J. Phys. Chem. B* **2004**, *108*, 2998−3004.
(46) Pankove, J. I. *Optical Processes in Semiconductors*; Dover: New York, 1975.
(47) Berger, T.; Sterrer, M.; Diwald, O.; Knozinger, E.; Panayotov, D.; Thompson, T. L.; Yates Jr., J. T. *J. Phys. Chem. B*, in press.
(48) Lamont, C. L. A.; Conrad, H.; Bradshaw, A. M. *Surf. Sci.* **1993**, *287*, 169−174.
(49) Zhou, X. L.; White, J. M. Photodissociation and Photoreaction of Molecules Attached to Metal Surfaces. In *Laser Spectroscopy and Photo-Chemistry on Metal Surfaces*; Dai, H.-L., Ho, W. K., Eds.; World Scientific Publishing Co.: River Edge, NJ, 1995; Vol. 5, pp 1141−1240.
(50) Roop, B.; Lloyd, K. G.; Costello, S. A.; Campion, A.; White, J. M. *J. Chem. Phys.* **1989**, *91*, 5103−5114.
(51) Marsh, E. P.; Gilton, T. L.; Meier, W.; Schneider, M. R.; Cowin, J. P. *Phys. Rev. Lett.* **1988**, *61*, 2725−2728.
(52) Holbert, V. P.; Garrett, S. J.; Stair, P. C.; Weitz, E. *Surf. Sci.* **1996**, *346*, 189−205.
(53) Linsebigler, A.; Lu, G. Q.; Yates Jr., J. T. *J. Phys. Chem.* **1996**, *100*, 6631−6636.
(54) Mezhenny, S.; Maksymovych, P.; Thompson, T. L.; Diwald, O.; Stahl, D.; Walck, S. D.; Yates Jr., J. T. *Chem. Phys. Lett.* **2003**, *369*, 152−158.